analytical chemistry

Article

pubs.acs.org/ac

# Multivariate Analysis for Quantification of Plutonium(IV) in Nitric Acid Based on Absorption Spectra

Amanda M. Lines,* Susan R. Adami, Sergey I. Sinkov, Gregg J. Lumetta, and Samuel A. Bryan*

Energy and Environment Directorate, Pacific Northwest National Laboratory, Richland, Washington 99352, United States

Supporting Information

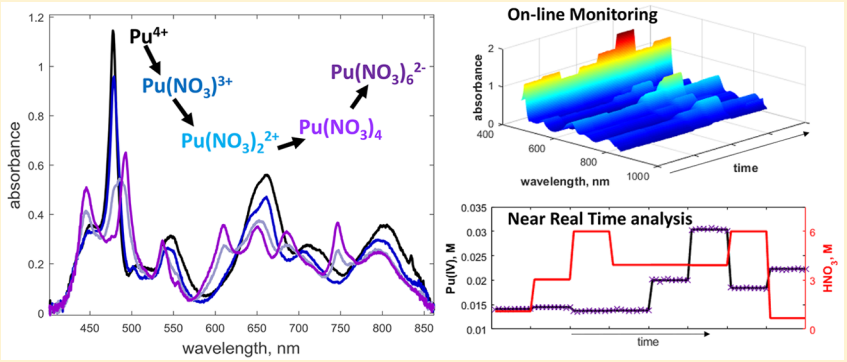


**ABSTRACT:** Development of more effective, reliable, and fast methods for monitoring process streams is a growing opportunity for analytical applications. Many fields can benefit from online monitoring, including the nuclear fuel cycle where improved methods for monitoring radioactive materials will facilitate maintenance of proper safeguards and ensure safe and efficient processing of materials. Online process monitoring with a focus on optical spectroscopy can provide a fast, nondestructive method for monitoring chemical species. However, identification and quantification of species can be hindered by the complexity of the solutions if bands overlap or show condition-dependent spectral features. Plutonium(IV) is one example of a species which displays significant spectral variation with changing nitric acid concentration. Single variate analysis (i.e., Beer's Law) is difficult to apply to the quantification of Pu(IV) unless the nitric acid concentration is known and separate calibration curves have been made for all possible acid strengths. Multivariate or chemometric analysis is an approach that allows for the accurate quantification of Pu(IV) without a priori knowledge of nitric acid concentration.

Common spectrophotometric techniques, such as absorption spectroscopy, are often utilized for fast and nondestructive qualitative and quantitative sample analysis. However, application of absorption spectroscopy and similar techniques is often limited by the difficulties imposed by interfering absorption bands, shifting baselines, or spectral dependencies on solution conditions. Traditional single variate forms of analysis, such as Beer's Law, will often fail under these conditions without a priori knowledge of solution conditions or the interfering species present.

Advances in mathematical approaches to data analysis are opening new avenues for the characterization of complex solutions, while utilizing techniques, such as absorption spectroscopy. Multivariate analysis, often referred to as chemometric analysis in these applications, allows for the utilization of the entire spectrum (instead of a single wavelength) for the quantification of species in solution.[1] This approach has been successfully used to quantify neodymium in both aqueous and organic solutions in solvent extraction systems, measure pH in weak acid systems (based on Raman spectra), quantify strong acids in solution, and quantify lanthanides in molten salt.[2−6]

Many systems exhibit the complex behavior that makes single variate analysis difficult, but in this Article, we focus on Pu(IV) and nitric acid ($HNO_3$) solutions. Quantifying Pu(IV) is important in nuclear materials processing, especially with regards to safeguarding and accounting of Pu,[7] safely operating processing facilities,[2] and safely storing Pu-containing materials.[8] Purified Pu(IV) is often processed in $HNO_3$.[9] Within these systems Pu(IV) will exhibit dynamic acid-concentration-dependent speciation that drastically affects the spectral fingerprint of Pu(IV). Despite the strong and well-known Pu(IV) absorption bands, this severe spectral variation makes single-variate quantification of the Pu difficult without first quantifying $HNO_3$, which can substantially slow down analysis.

Here, we discuss the application of chemometric analysis to the successful quantification of Pu(IV) based on absorption spectra. For this analysis, prior knowledge of $HNO_3$ concentration is not required. Chemometric models can be built based on a training set of Pu(IV) spectra collected across a

**Received:** June 6, 2017
**Accepted:** July 20, 2017
**Published:** July 20, 2017





DOI: 10.1021/acs.analchem.7b02161
*Anal. Chem.* 2017, 89, 9354−9359

range of $HNO_3$ concentrations. These models can then be used to accurately identify and quantify Pu(IV) in new or unknown samples. Recent studies have opened the door for this type of mathematical approach,[10] and here, we explore new approaches while connecting solution chemistry to the explanation of model outputs.

## EXPERIMENTAL SECTION

**Materials.** Reagent grade concentrated nitric acid was obtained from Sigma-Aldrich and was used as received. Nitric acid solutions were made by diluting in 18 MΩ pure water and concentrations were verified by titration.

The plutonium stock solution was generated from solid Pu (239, 240) oxide and reconstituted in 4 M nitric acid to prevent hydrolysis and generally maintain Pu in the 4+ oxidation state. Stock solution concentration was checked regularly using a secondary UV−vis system, and values were corroborated using the primary spectroscopic system utilized in the collection of the training set data. While there is always some uncertainty in measured Pu concentration, noted values for Pu concentration in the training set were corrected based on checked Pu stock concentration.

In this study, Pu was only studied at 0.5 M $HNO_3$ and above to limit hydrolysis of Pu(IV).[11−13] It should also be noted that under the conditions here, Pu(IV) displayed limited disproportionation to Pu(III) and Pu(VI) as can be expected at some low acid conditions.[14] Further discussion of this can be found in the Supporting Information.

**Equipment.** Spectra were collected using a UV−vis spectrometer from Spectra Solutions, Inc., and associated Spectra Soft software. Reference spectra were collected on pure water and integration times were 0.2 s. Quartz cuvettes with a 1 cm path length were utilized.

While not utilized here, it should be noted that cuvettes with shorter path lengths could be used to explore Pu systems at higher Pu concentrations.

**Chemometric Modeling.** All chemometric models were generated using Eigenvector Research PLS toolbox for MATLAB (version R2015B utilized here). Details on model types, numbers of principal components, and model performance parameters are included in the discussion.

The calibration set included 1100 UV−vis spectra corresponding to 110 samples (10 spectra per sample). The 110 samples included a series of Pu solutions ranging from 0 to 33 mM repeated at 0.5 to 10 M $HNO_3$. Cross validation (when used) utilized the venetian blinds approach to remove sets of spectra (10 per sample) associated with random samples. The validation set included an entirely separate set of spectra of Pu in $HNO_3$. A total of 80 spectra were included with 10 spectra collected for each sample.

## RESULTS AND DISCUSSION

The UV−vis absorption spectroscopy of Pu(IV) is known to vary significantly based on solution composition and Pu speciation.[11,14−17] Of particular interest to this work is the spectral variation observed across a range of $HNO_3$ concentrations, which can be seen in the top plot of Figure 1. Figure 1 also includes pictures of a roughly 0.07 M Pu solution in 1, 5, and 10 M $HNO_3$. In the range of 0.5 to 5 M $HNO_3$ the Pu solution remains a yellow brown color. Above 5 M $HNO_3$, the Pu solution shifts to a bright green color.

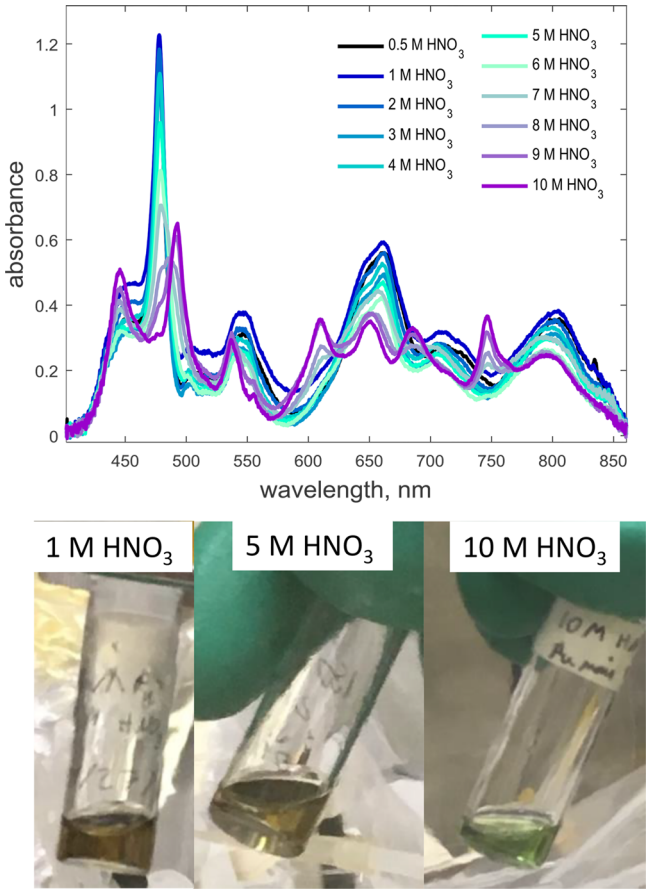


**Figure 1.** (Top) Spectra of 15 mM Pu in $HNO_3$ ranging from 0.5 to 10 M. (Bottom) Pictures of Pu solutions at different $HNO_3$ concentrations.

The spectral variation exhibited in Figure 1 is due to the formation of multiple Pu−nitrato complexes. This includes the fully hydrated, mononitrato, dinitrato, tetranitrato, and hexanitrato species. This complex speciation leads to the increased difficulty in quantifying Pu in solutions where the $HNO_3$ concentration is unknown. The degree to which band shapes and molar extinction coefficients change is demonstrated by the absorbance versus concentration plots in Figure 2, captured at 1, 5, and 10 M $HNO_3$. Beer's Law plots for other acid concentrations (0.5, 2, 3, 4, 6, 7, 8, and 9 M) are presented in the Supporting Information. Table 1 lists the molar extinction coefficients for the major Pu(IV) band in the range of 450−500 nm for all $HNO_3$ concentrations studied. Data for other acid strengths is included in the Supporting Information. It should be noted that the UV−vis instrument used for this application sacrificed higher resolution for higher sensitivity; this limits the wavelengths measured and results in peak maxima and molar extinction coefficients that differ slightly from what is reported by other authors. With this in mind, observed results fall within the range of values described in literature.[16,18] Molar extinction coefficients were calculated from the slope of the absorbance vs concentration curves (for the linear response range). The estimated error in the slope of the line is included to indicate the uncertainty of the molar extinction coefficients.

The spectral complexity and the peak variation highlighted in Figures 1 and 2 and in Table 1 indicate traditional single variate analysis (Beer's Law) represents a difficult path for quantifying



DOI: 10.1021/acs.analchem.7b02161
Anal. Chem. 2017, 89, 9354−9359

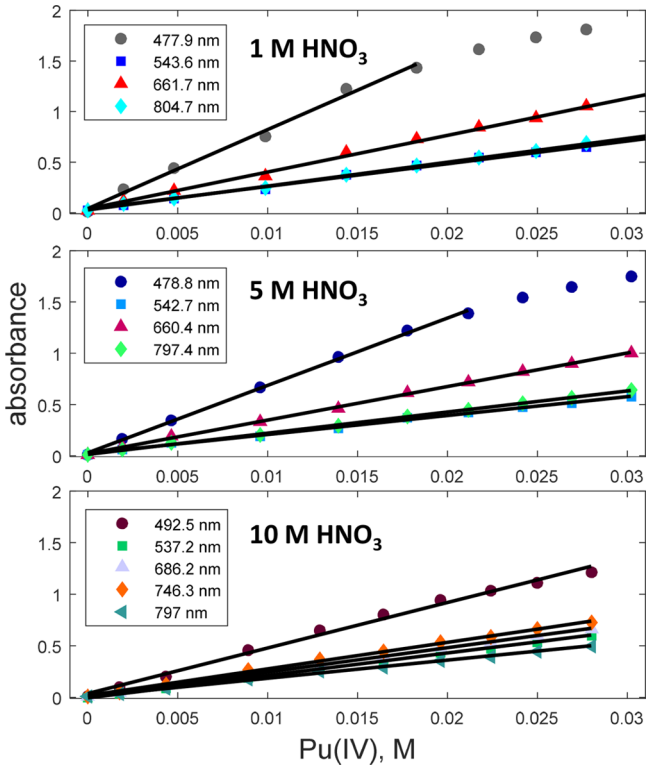


**Figure 2.** Beer's Law plots for the major Pu 4+ bands at 0.5 M $HNO_3$(top), 5 M $HNO_3$ (middle), and 10 M $HNO_3$ (bottom). Best fit lines are shown in black.

**Table 1. Molar Absorptivities of Pu(IV) Band in the 450–500 nm Range as a Function of $HNO_3$ Concentration**

| $HNO_3$ (M) | $\lambda_{max}$ (nm) | $\varepsilon$ ($cm^{-1}$ $M^{-1}$) | $R^2$ | linear Pu range (M) |
|---|---|---|---|---|
| 0.5 | 477.5 | 64 (±2) | 0.995 | 0–0.022 |
| 1 | 477.9 | 78 (±3) | 0.993 | 0–0.018 |
| 2 | 477.9 | 77 (±6) | 0.973 | 0–0.020 |
| 3 | 478.3 | 73 (±2) | 0.998 | 0–0.020 |
| 4 | 478.3 | 72 (±4) | 0.990 | 0–0.020 |
| 5 | 478.8 | 65 (±1) | 0.999 | 0–0.022 |
| 6 | 478.8 | 58.8 (±0.8) | 0.999 | 0–0.022 |
| 7 | 479.6 | 49.9 (±0.3) | 0.999 | 0–0.022 |
| 8 | 485.2 | 39.5 (±0.4) | 0.999 | 0–0.025 |
| 9 | 490.8 | 40.9 (±0.7) | 0.993 | 0.0.028 |
| 10 | 492.5 | 44 (±1) | 0.993 | 0–0.028 |

Pu(IV) in solution. This has been recognized and initial developments in multivariate approaches to quantifying Pu have been published including systematic treatment of select wavelengths[19,20] and PLS regression techniques that break down acid strength regions to apply multiple hierarchical models.[10] However, advances in mathematical approaches to data analysis have opened up new routes for quantifying species under complex conditions. Chemometric analysis allows for the utilization of the entire spectrum (instead of a single wavelength) for the quantification of species in solution.[1,21] Chemometric analysis utilizes spectral training sets to find covariance between spectral data sets and corresponding concentration matrices. To accurately identify and quantify analytes, chemometric models must be built using training sets that capture the full range of anticipated solution conditions (e.g., analyte concentration or interfering species). For this work, spectra of Pu(IV) at 0–30 mM in 0.5–10 M $HNO_3$ were utilized as the training set for model development. This represents a system where only the matrix effects ($HNO_3$ affecting Pu(IV) spectral response) are explored. Different spectral interferences are observed in systems containing other interfering species (e.g., Pu(III), Pu(VI), U, or other fission products). Multicomponent systems will be explored in more detail in future work.

Multivariate curve resolution (MCR) can be used to model the spectral influences of the various Pu(IV)–nitrate complexes and provide speciation information. This approach differs from, but is complementary to, approaches utilized by HypSpec and similar software packages.[22] Figure 3 depicts the MCR

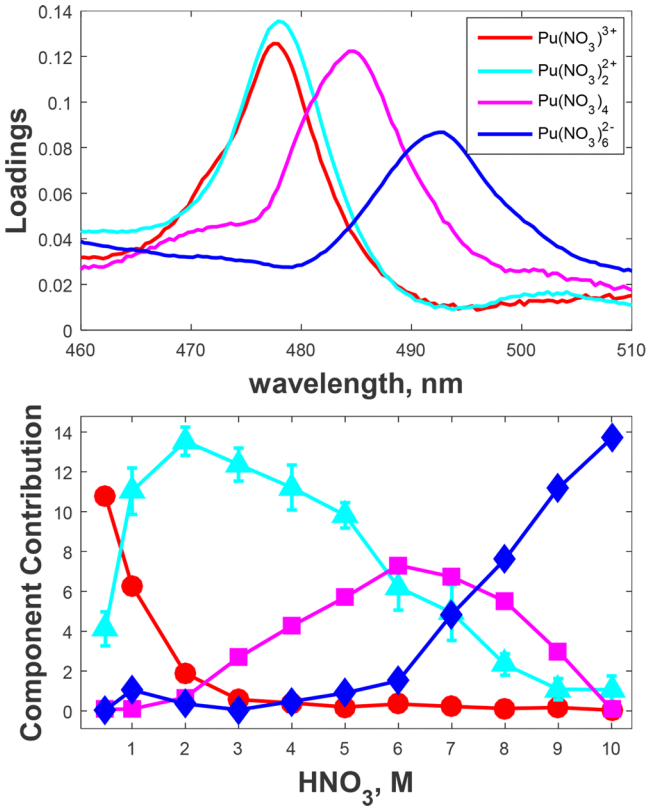


**Figure 3.** (Top) MCR loadings corresponding to the spectral influences of the various Pu–nitrate complexes. (Bottom) Pu speciation as a function of $HNO_3$ determined via MCR modeling. The *y* axis corresponds to influence of the principal components (top plot) in the calculation of Pu concentration. Both plots utilize the legend in the top plot.

modeling results which break down the spectral components of each Pu–nitrate complex (top). Figure 3 (bottom) also indicates which component has the highest model loadings as a function of $HNO_3$ to provide what is essentially a speciation diagram. Numerous studies have been completed to determine Pu speciation in $HNO_3$ solutions. In general, most agree that a fully hydrated complex will exist in sufficiently dilute $HNO_3$ and a hexanitrato complex will predominate in solution above 10 M $HNO_3$.[16,23,24] However, because of the lack of true isosbestic points and confounded band behaviors, the mononitrato, dinitrato, and tetranitrato effects have been a source of contention among Pu chemists.[25–27] Recent work has reached consensus on the stability constant of the mononitrato complex.[28] Thermodynamic modeling can be utilized to model


DOI: 10.1021/acs.analchem.7b02161
*Anal. Chem.* 2017, 89, 9354–9359

Pu solutions containing the aquo-, mono-, and dinitrato species[29] or the di-, tetra-, or hexanitrato species.[26] The mono and dinitrato species have been isolated via mixed acid titrations.[25] The tetranitrato species spectral signature has been isolated using systematic analysis of Pu(IV) spectra in varied $HNO_3$ and also through NMR and EXAFS analysis.[27,30,31]

The MCR modeling results align with what has been reported in the literature given slight differences in the wavelength of peak maxima, which can be attributed to the resolution of the instrument used. The mononitrato and dinitrato species have been identified as having confounding bands at 476 nm.[23,27] MCR results capture and isolate the variance associated with the mono and dinitrato species with two bands at 477.5 nm. The tetranitrato species has a major absorption band at 483 nm and hits a maximum concentration at 8 M $HNO_3$.[23,27,31] The MCR model identified this species with a band at 484.3 nm and notes the species hits a maximum at approximately 7 M $HNO_3$. This observed maximum in the 6−7 M $HNO_3$ range correlates well with speciation plots produced by some groups.[32] The hexanitrato species exhibits a maximum absorbance at 491 nm and dominates the speciation profile above 10 M $HNO_3$.[27,31] This, again is accurately calculated by the model with a band at 492.5 nm identifying the species that dominates the speciation profile above 10 M $HNO_3$.

The model has difficulty identifying and isolating the effects of the fully hydrated species. This is most likely due to the very low concentrations of the fully hydrated complex anticipated under the conditions studied here. The aquo complex band should appear at 469 nm as has been observed in perchloric acid systems.[16,17,27] The MCR model presented here captures this species as a shoulder at 470 nm but confounds this band with the mononitrato complex. Given the low concentrations anticipated for the aquated species, it is impressive the model captured the 470 shoulder at all. It is possible that this issue could be resolved by adding spectra of the aquated species to the training set. Spectra of Pu(IV) in perchloric acid systems would be ideal but were not included here as perchloric acid conditions do not align with overall project interests. Additionally, the model breaks the dinitrato complex into 2 components in order to deconvolute the dinitrato species from the mononitrato species. Figure 3 shows the results of coadding the 2 components capturing the dinitrato species while the uncorrected data is shown in the Supporting Information.

Note, the fully hydrated species is fully confounded with the mononitrato species. As a result the bottom plot of Figure 3 primarily indicates component contribution for the mononitrato species. According to other reports, the fully aquated species should represent less than 20% of the Pu at 0.5 M $HNO_3$ and roughly 0% above that. Again, the *y* axis of the bottom plot is not species percent but an arbitrary scale representing model weightings.

MCR results align well with what has been reported in the literature, indicating that MCR results are accurate and that MCR represents a viable route for exploring the speciation of solution based systems. It should also be noted that model constraints such as identifying acid ranges where only one Pu(IV) species would be present were explored but not utilized for the data presented here. Adding forced constraints did not drastically change results and the high level of accuracy exhibited by MCR results without forced constraints presents a strong argument for the utility of this technique.

In general, MCR analysis is helpful in providing examples of how other forms of chemometric software are applied. Spectral data is simplified by representing variables (e.g., spectral data) as vectors within a 3D space. With all the training set in place, new vectors can be identified that capture the primary vector direction of the data. In this way, wavelength regions where the greatest variation is observed are identified and used to produce a model where principal components (loadings or latent variables here) are used to express those regions of spectral variation. The mathematical operations/approaches vary with the type of modeling utilized, where different models have different output goals (i.e., classification, speciation, quantification, etc.).[1,10,33−36]

Figure 4 presents the observed loadings for a locally weighted regression (LWR) model produced from the same spectral training set used for the MCR modeling above. In this case, LWR is focused on quantifying the total Pu(IV) present as opposed to breaking down the speciation, as was the goal with the MCR model. The LWR model utilizes a nonlinear approach to calculating species concentration which is particularly powerful under the conditions of the Pu system studied here. Specifically, Pu concentrations extend to 33 mM, which is above the 20 mM cutoff for linear Beer's Law plots at some acid strengths. Additionally, Pu(IV) exhibits significant spectral variation across the $HNO_3$ range studied. Loadings were calculated after applying a first derivative to the data, which emphasizes the areas of spectral change. Loadings are broken into components indicating their order of importance to the model calculations of Pu concentration and indicate which spectral regions are highly correlated to Pu signatures.

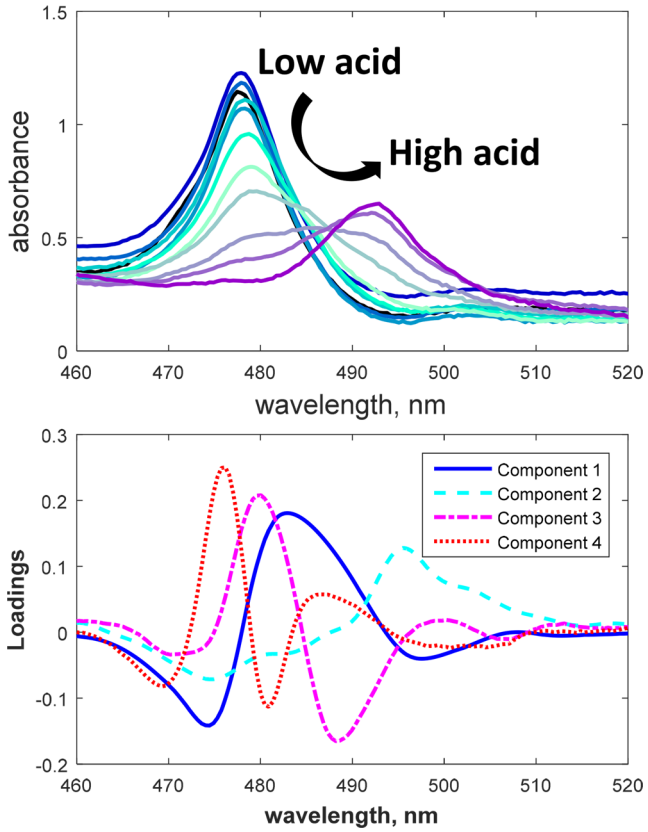


**Figure 4.** (Top) Pu(IV) spectra as $HNO_3$ concentration is varied, see legend in Figure 1. (Bottom) Loadings produced by LWR modeling.



DOI: 10.1021/acs.analchem.7b02161
*Anal. Chem.* 2017, 89, 9354−9359

Figure 4 presents the loadings, where component 1 captures the general Pu(IV) band in the 470−500 nm range as being positively related to Pu(IV) concentration. This broad loading positively captures the spectral influences of all 5 Pu species with a slight negative dip which captures the general shift of the band. Component 2 captures the ingrowth of the band corresponding to the hexanitrato complex as being positively related to Pu(IV) concentration. Component 3 shows a positive loading at 480 nm which drops to a negative loading at 488 nm; this captures the tetranitrato species as well as the observed shift of the band in the range of 5−8 M $HNO_3$. Similar to component 3, component 4 captures the gradual band shift observed in the range of 1−5 M $HNO_3$, as well as the positive contributions of the confounded mono- and dinitrato species. Note that areas of little importance (e.g., 510−520 nm) have low magnitude loadings (nearing 0), while areas of importance are given higher magnitude loadings.

The LWR model performance is demonstrated in Figure 5, which plots the Pu(IV) concentrations calculated by the model

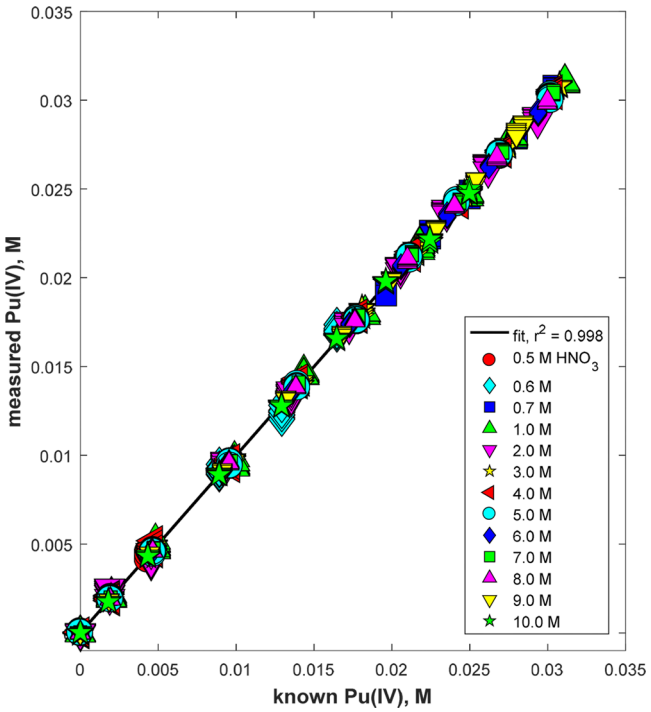


**Figure 5.** Measured (by LWR modeling) Pu(IV) concentration as a function of known Pu(IV) concentration. Data points are class colored by $HNO_3$ concentration.

versus the known Pu(IV) concentrations of the model training set. Data points are class colored to indicate the $HNO_3$ concentration of the Pu samples. The calculated concentrations show a one-to-one correlation with known values for the full range of $HNO_3$ signifying excellent model performance. The spectral data were preprocessed using a first derivative followed by a mean center to address any baseline issues and emphasize areas of primary variation. The model was cross validated by pulling out all spectra of random samples from the calibration set and subsequently treating that data as a validation set. The cross validation offers a route to test how the model will perform on unknown (i.e., not a part of the training set) spectra. The root-mean-square error (RMSE) of the model (RMSEC) was 0.00017, and for the cross validation (RMSECV) was 0.00041. These values can be roughly interpreted as ±errors in calculated concentrations. Because these values are low and errors for the model are similar to errors for the cross validation, this model is both accurate and robust enough to operate successfully on unknown samples. Figure S13 provides a zoomed-in view of a portion of Figure 5 to allow for easier viewing of the density of the data points.

To fully test the model performance, it is necessary to apply the model to spectra of truly unknown (to the training set) samples. Models capable of accurately measuring the concentration of species based on spectra not contained in the training set are considered robust and capable of effective quantification. Figure 6 presents a series of spectra of Pu(IV)

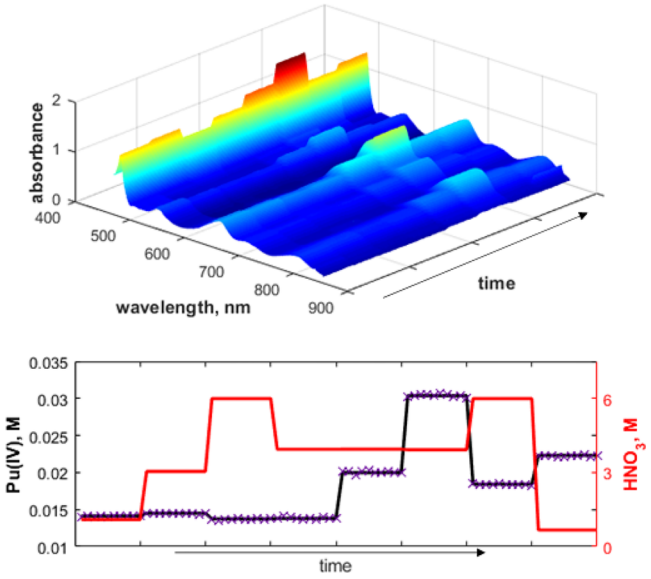


**Figure 6.** (Top) spectral response over a series of samples as Pu(IV) and $HNO_3$ are varied. (Bottom) known values of Pu(IV) (black line) and $HNO_3$ (red line, red axis) with chemometric measurements of Pu(IV) (purple markers).

solutions at varying $HNO_3$ concentrations that were not included in the LWR training set. The bottom plot shows how the calculated values (from the LWR model) compare to the known concentrations of the system. A model for $HNO_3$ concentration based on the Pu UV−vis spectral response is achievable and will be the subject of future papers.

As demonstrated by Figure 6, the LWR model successfully measures Pu concentrations in all samples. Under conditions where Pu is held constant, while $HNO_3$ is varied, vice versa, and when both components are varied simultaneously, the chemometric model accurately follows the Pu concentration. The root-mean-square error of prediction was 0.0002 (which can be interpreted as ±0.0002 M) indicating accurate measurement of Pu(IV) concentration. Additional meta data, such as Q residuals, indicated low error with the model accurately representing the spectral response observed in the flow test. It is again important to note that all measurements made by the chemometric model were based on UV−vis absorbance spectra only, the model has no information regarding acid strength. This represents a major step forward for quantifying Pu, or any analyte exhibiting acid-dependent spectra, under complex solution conditions.



DOI: 10.1021/acs.analchem.7b02161
Anal. Chem. 2017, 89, 9354−9359

## CONCLUSIONS

Plutonium(IV) exhibits complex speciation as a function of $HNO_3$ concentration, which leads to significant variations in absorption spectra. Despite this spectral complexity, chemometric modeling can be successfully utilized to follow Pu speciation as a function of $HNO_3$ with multivariate curve resolution modeling. Additionally, locally weighted regression models can be deployed to accurately quantify Pu(IV) in solution without first quantifying $HNO_3$. Overall, chemometric analysis offers a highly successful approach to quantifying Pu even under complex conditions. This represents a significant improvement in spectral analysis where systems that cannot be quantified using single variate analysis can now be effectively characterized. Utilizing this quantification approach can greatly expand the utility of common spectrophotometric techniques.

## ASSOCIATED CONTENT

### Supporting Information

The Supporting Information is available free of charge on the ACS Publications website at DOI: 10.1021/acs.analchem.7b02161.

Supplemental data, calibration curves for the primary Pu(IV) peaks, Pu(IV) bands, MCR loadings corresponding to the spectral influences of the various Pu−nitrate complexes, Pu speciation as a function of $HNO_3$, and a close up of Figure 5 (PDF)

## AUTHOR INFORMATION


### Corresponding Authors

*E-mail: amanda.lines@pnnl.gov.
*E-mail: sam.bryan@pnnl.gov. Phone: (509) 375-5648.

### ORCID

Samuel A. Bryan: 0000-0002-8826-0880


### Notes

The authors declare no competing financial interest.

## ACKNOWLEDGMENTS

Research was supported by U.S. Department of Energy, Office of Nuclear Energy, through the Nuclear Technologies R&D Program, as well as the Department of Homeland Security, and was performed at the Pacific Northwest National Laboratory (PNNL) operated by Battelle for the U.S. Department of Energy under Contract DE-AC05-76RL01830.

## REFERENCES


(1) Beebe, K. R.; Pell, R. J.; Seasholtz, M. B. *Chemometrics: A Practical Guide*; Wiley: New York, 1998.
(2) Bryan, S. A.; Levitskaia, T. G.; Casella, A. J.; Peterson, J. M.; Johnsen, A. M.; Lines, A. M.; Thomas, E. M. In *Advanced Separation Techniques for Nuclear Fuel Reprocessing and Radioactive Waste Treatment*; Nash, K. L., Lumetta, G. J., Eds.; Woodhead Publishing: Cambridge, UK, 2011; pp 95−119.
(3) Bryan, S. A.; Levitskaia, T. G.; Johnsen, A. M.; Orton, C. R.; Peterson, J. M. *Radiochim. Acta* **2011**, *99*, 563−571.
(4) Casella, A. J.; Ahlers, L. R. H.; Campbell, E. L.; Levitskaia, T. G.; Peterson, J. M.; Smith, F. N.; Bryan, S. A. *Anal. Chem.* **2015**, *87*, 5139−5147.
(5) Casella, A. J.; Levitskaia, T. G.; Peterson, J. M.; Bryan, S. A. *Anal. Chem.* **2013**, *85*, 4120−4128.
(6) Schroll, C. A.; Lines, A. M.; Heineman, W. R.; Bryan, S. A. *Anal. Methods* **2016**, *8*, 7731−7738.
(7) Burr, T.; Budlong-Sylvester, K.; Myers, K.; Demuth, S.; Bakel, A.; Krebs, J.; Bryan, S.; Orton, C.; Ehringer, M.; Garcia, H. *JNMM—Journal of the Institute of Nuclear Materials Management* **2012**, *40*, 42.
(8) Orton, C.; Bryan, S.; Schwantes, J.; Levitskaia, T.; Fraga, C.; Peper, S. In *Proceedings of the Symposium on International Safeguards*, Vienna, Austria; 2010.
(9) Herbst, R. S.; Baron, P.; Nilsson, M. In *Advanced Separation Techniques for Nuclear Fuel Reprocessing and Radioactive Waste Treatment*; Nash, K. L.; Lumetta, G. J., Eds.; Woodhead Publishing, 2011; pp 141−175.
(10) Lascola, R. J.; O'Rourke, P. E.; Kyser, E. A.; Immel, D. M.; Plummer, J. R.; Evans, E. V. *Spectrophotometers for Plutonium Monitoring in HB-Line*, SRNL-STI-2015-00454; Savannah River National Laboratory, 2016.
(11) Weigel, F.; Katz, J. J.; Seaborg, G. T. In *The Chemistry of the Actinide Elements*; Katz, J. J., Seaborg, G. T., Morss, L. R., Eds.; Chapman and Hall: New York, 1986.
(12) Walther, C.; Cho, H. R.; Marquardt, C. M.; Neck, V.; Seibert, A.; Yun, J. I.; Fanghanel, T. *Radiochim. Acta* **2007**, *95*, 7−16.
(13) Yun, J. I.; Cho, H. R.; Neck, V.; Altmaier, M.; Seibert, A.; Marquardt, C. M.; Walther, C.; Fanghanel, T. *Radiochim. Acta* **2007**, *95*, 89−95.
(14) Metz, C. F. *Anal. Chem.* **1957**, *29*, 1748−1756.
(15) Cohen, D. *J. Inorg. Nucl. Chem.* **1961**, *18*, 211−218.
(16) Connick, R. E.; Kasha, M.; McVey, W. H.; Sheline, G. E. In *The Transuranium Elements*; Seaborg, G. T., Katz, J. J., Manning, W. M., Eds.; McGraw-Hill Book Company: New York, 1949; p 559.
(17) Hindman, J. C. In *The Transuranium Elements*; Seaborg, G. T., Katz, J. J., Manning, W. M., Eds.; McGraw-Hill Book Company: New York, 1949; p 370.
(18) Hagan, P. G.; Miner, F. J. *Spectrophotometric Determination of Plutonium III, IV, and VI in Nitric Acid Solutions*; Dow Chemical Company: Golden, CO, 1969.
(19) Baumgärtel, G.; Kuhn, E. *Anal. Chim. Acta* **1971**, *53*, 208.
(20) Schmieder, H.; Kuhn, E. *Chem. Ing. Tech.* **1972**, *44*, 104.
(21) Workman, J.; Lavine, B.; Chrisman, R.; Koch, M. *Anal. Chem.* **2011**, *83*, 4557−4578.
(22) Gallagher, N. B.; Blake, T. A.; Gassman, P. L.; Shaver, J. M.; Windig, W. *Appl. Spectrosc.* **2006**, *60*, 713−722.
(23) Hindman, J. C. In *The Transuranium Elements*; Seaborg, G. T., Katz, J. J., Manning, W. M., Eds.; McGraw-Hill Book Company, Inc.: New York, 1949; p 388.
(24) Ryan, J. L. *J. Phys. Chem.* **1960**, *64*, 1375−1385.
(25) Berg, J. M.; Veirs, D. K.; Vaughn, R. B.; Cisneros, M. A.; Smith, C. A. *J. Radioanal. Nucl. Chem.* **1998**, *235*, 25−29.
(26) Kubic, W. L.; Jackson, J. C. *J. Radioanal. Nucl. Chem.* **2012**, *293*, 601−612.
(27) Veirs, D. K.; Smith, C. A.; Berg, J. M.; Zwick, B. D.; Marsh, S. F.; Allen, P.; Conradson, S. D. *J. Alloys Compd.* **1994**, *213*, 328−332.
(28) Lemire, R. J. *Chemical Thermodynamics of Neptunium and Plutonium*; OECD Nuclear Energy Agency, Eds.; Elsevier Science: Amsterdam, The Netherlands, 2001; pp 405−406.
(29) Berg, J. M.; Veirs, D. K.; Vaughn, R. B.; Cisneros, M. R.; Smith, C. A. *Appl. Spectrosc.* **2000**, *54*, 812−823.
(30) Allen, P. G.; Veirs, D. K.; Conradson, S. D.; Smith, C. A.; Marsh, S. F. *Inorg. Chem.* **1996**, *35*, 2841−2845.
(31) Marsh, S. F.; Day, R. S.; Veirs, D. K. *Spectrophotometric Investigation of the Pu(IV) Nitrate Complex Sorbed by Ion Exchange Resins*; Los Alamos National Laboratory, 1991.
(32) Barr, M. E.; Jarvinen, G. D.; Moody, E. W.; Vaughn, R.; Silks, L. A.; Bartsch, R. A. *Sep. Sci. Technol.* **2002**, *37*, 1065−1078.
(33) Bro, R.; Elden, L. *J. Chemom.* **2009**, *23*, 69−71.
(34) Höskuldsson, A. *J. Chemom.* **1988**, *2*, 211−228.
(35) Cleveland, W. S.; Devlin, S. J. *J. Am. Stat. Assoc.* **1988**, *83*, 596−610.
(36) Ruppert, D.; Wand, M. P. *Ann. Stat* **1994**, *22*, 1346−1370.




DOI: 10.1021/acs.analchem.7b02161
*Anal. Chem.* 2017, 89, 9354−9359